Proc. of JSCE,
No. 184, Dec. 1970

ESTIMATION OF SAFE SPACING AMONG VERTICAL LINES IN OCEAN

*Masaru Hoshiya**
*Theodore Zsutty***

I. INTRODUCTION

This paper provides a probabilistic method of estimating safe spacing among vertical lines in the ocean. To improve the performance of a conventional flexible hoisting line with an equipment for oceanographic surveys, ropes stretched vertically in the ocean between buoys and anchors have been proposed as a guidance system for the weight hoisting line[1]. The schematic system is illustrated in Fig. 1. The hoisting line is parallel with the guide cables. For a safe operation, horizontally provided is a rope which connects the three vertical lines. The system may consist of either steel wire ropes or neutrally buoyant synthetic lines.

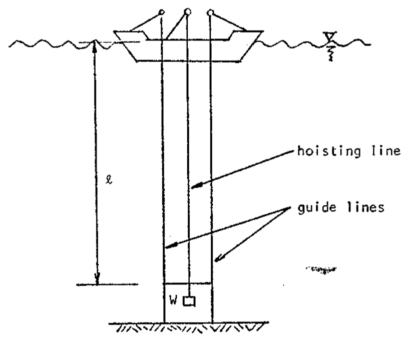

Fig. 1 Schematic Hoisting System

Questions have been raised about the safety of the system under hostile ocean environment. The hoisting line will tend to entangle (touch) with the guide lines if these lines are not sufficiently separated and if these lines are long. This study will determine the minimum safe spacing between the ocean surface ends of lines by employing random vibration theory.

The possible sources of system excitation are surface wave actions, subsurface currents and turbulence force. The ship will be subjected to vertical and horizontal displacements due to surface waves or sea swell action. The vertical displacement may be modeled as a sinusoidal vertical motion of the top boundary condition provided by a ship, where the frequency and amplitude are constant values typical of the operational sea environment. In the mathematical model, this vertical motion would have the effect of creating a sinusoidal time variation in the line tension. This effect on the lateral displacement of the system is separately treated. This may then be superimposed onto the results due to the other excitations.

The cables are assumed to be stretched vertically. In reality, cables do not hang directly beneath the surface buoy boundary. They are deflected by the force of currents at depth and by the drift of the ship on the surface and this

* Assistant Professor of Engineering Mechanics, Virginia Polytechnic Institute and State University.
** Professor of Civil Engineering and Applied Mechanics, San Jose State College.

causes in general, a catenary shape of the lines[2]. This current is assumed to be a non-time varying constant force. Thus, the portion of the horizontal displacement due to the constant current force is a deterministic hydrostatic problem which depends on rope size and tension, and on buoy and suspended weight size and shape. If parallel ropes have different constant displacements due to the current, then this difference must be included in the minimum safe distance between surface buoys. This effect, however, is not included in this analysis, since it is possible that the system is arranged so as to have nearly equal response to this steady current. For example, nearly equal tensions and weights should be employed. We also assume the effect of the drift of a ship is negligible compared to the long vertical lines.

Turbulence force is most critical just after a big storm. The dispersion of this force is great in general, and therefore, the turbulence force is assumed to be a stationary normal random process with a known spectral density function and with zero mean. Wave force effect near the surface is taken to be included in this force.

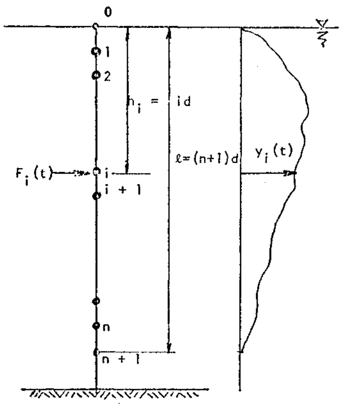

Fig. 2 Lumped-parameter Model

For the theoretical analysis, the vertical line is to be modeled as a lumped-parameter system subjected to turbulence forces $F_i(t)$ at lumped mass locations i, having horizontal displacements $y_i(t)$—Fig. 2. The complete random description of $F_i(t)$ can be provided in terms of a given cross-spectral density function matrix. The boundary condition for a floating buoy cannot be zero in its horizontal displacement. However, we assume $y_0(t)\equiv 0$. This is due to our previously described assumption of the small drift of a ship.

The analysis which follows next was performed for co-planar motion. The real problem is a three dimensional one, such as wave spectra, turbulence spectra, etc. However, for a conservative estimation of safe spacing, co-planar analysis is employed.

II. TURBULENCE FORCE

The dispersion of the turbulence force near the surface is naturally great and will be reduced with the depth level. Consequently, the variance C_{ii} or mean squared value of the turbulence force $F_i(t)$ at an instant t, about its zero mean value, is assumed to have a linear variation with depth level i. The covariance C_{ij} between the turbulence forces $F_i(t)$ and $F_j(t)$ is also assumed to have a linear variation with respect to the separation distance $(i-j)d$ where $i\geq j$.

$$C_{ii}=C_{11}\left\{1-(1-B)\frac{i-1}{n-1}\right\}, \qquad i=1, 2, \cdots, n \tag{1}$$

where C_{11} and B are input constants and $0\leq B\leq 1$. For instance, a value of $B=1$ gives $C_{ii}=C_{11}$, a uniform variation and $B=0$ gives $C_{ii}=C_{11}\frac{n-i}{n-1}$, a simple triangular variation. In the absence of actual measured data for the depth profile of mean squared, deep-sea turbulence, it is felt that Eq. (1) is generally enough to allow an engineering analysis of vertical line deflections. The assumed variance pattern corresponds to the maximum type of turbulence force that follows the surface disturbance of a large storm.

For the covariances, first consider the maximum type (post-storm) of turbulence condition which has covariance between the bottom and top points as follows

$$C_{n1}=DC_{nn} \quad \text{for} \quad 0 \leq D \leq 1\,. \tag{2}$$

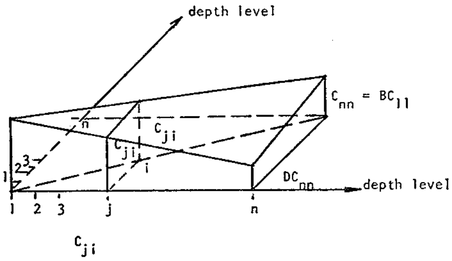

Fig. 3 Variance and Covariance of Turbulence Force

Since it has been assumed that the variance decreases with depth ($C_{jj} \leq C_{ii}$ for $i \leq j$), it is necessary to define covariance C_{ji} in terms of the smaller variance C_{jj} in order to avoid the impossible case of $C_{ji} > C_{jj}$. Thus, we have

$$C_{ji}=\frac{i-1}{j-1}C_{jj}+C_{11}\left[\frac{j-i}{j-1}-\frac{j-i}{n-1}\right]+DC_{nn}\frac{j-i}{n-1} \tag{3}$$

where $j=2, 3, \cdots, n$ and $i=1, 2, \cdots, j$. For a real valued force system, we have

$$C_{ji}=C_{ij}\,. \tag{4}$$

The $D=1$ case gives the maximum condition of perfect correlation and the $D=0$ case gives a zero correlation of the top force with the bottom force.

With the available expressions (1), (3), and (4), it is now necessary to define the frequency spectrum and cross-spectral density function of these variances. It is sufficient to define the cross-spectral density $S_{ij}(\omega)$ since it is able to include the case of $j=i$ required for $S_{ii}(\omega)$ and $S_{jj}(\omega)$.

For a real valued force system, we have

$$S_{ij}(\omega)=S_{ji}(\omega) \tag{5}$$

and a cross-spectral density function has the property of symmetry.

$$S_{ij}(-\omega)=S_{ij}(\omega)\,.$$

The spectrum $S_{ij}(\omega)$ is assumed to be a linear function of ω with a certain cut-off frequency ω_c beyond which no significant amplitude of frequency exists. Field data of turbulence forces or engineering judgement can provide this ω_c value (Fig. 4).

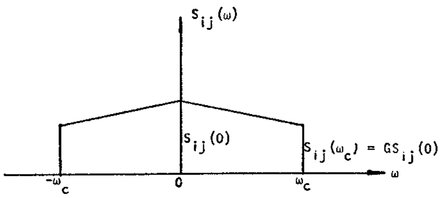

Fig. 4 Continuous Cross-Spectral Density Function

With the mathematical requirement that

$$C_{ij}=\int_{-\infty}^{\infty} S_{ij}(\omega)d\omega=\text{area under } S_{ij}(\omega) \tag{7}$$

we have

$$S_{ij}(\omega)=\frac{C_{ij}}{(1+G)\omega_c}\left\{1-(1-G)\frac{\omega}{\omega_c}\right\} \tag{8}$$

where G is a constant and $0 \leq G \leq 1$. Eq. (8) gives the relationship between co-variance and cross-spectral density function.

With Eq. (8), we can make the entire $(n \times n)$, symmetrical cross-spectral density function matrix for the turbulence force system $F_i(t)$. That is,

$$S_f = \begin{bmatrix} S_{11}(\omega), S_{12}(\omega), \cdots, S_{ij}(\omega), \cdots, S_{1n}(\omega) \\ S_{21}(\omega), S_{22}(\omega), \cdots \\ S_{i1}(\omega), S_{i2}(\omega), \cdots, S_{ij}(\omega), \cdots, S_{in}(\omega) \\ S_{n1}(\omega), S_{n2}(\omega), \cdots \qquad S_{nn}(\omega) \end{bmatrix}. \tag{9}$$

The discrete form of the cross-spectral density function is required for the numerical integration of $S_{ij}(\omega)$ in the reliability analysis later on. In order to obtain the discrete form, it is first necessary to select and assign the summation limit N, which will determine the frequency interval

$$\Delta\omega = \frac{\omega_c}{N}. \tag{10}$$

This N value should be large enough to describe adequately the curve of $S_{ij}(\omega)$. Then the expression of discrete cross-spectral density function is given by

$$S_{ij}(\omega)_D = \sum_{K=-N}^{N} S_{ij}(\omega_K)\Delta\omega\delta(\omega - \omega_K) \tag{11}$$

where $\omega_K = K\Delta\omega$ and $\delta(\omega - \omega_K)$ is the Dirac delta function.

III. DYNAMIC RESPONSE OF VERTICAL LINE SYSTEM

The reliability analysis of horizontal displacement requires a knowledge of the free vibration mode shapes and frequencies for the vertical line system shown in Fig. 1 or in Fig. 2. The upper boundary is assumed to be fixed at the water surface level as indicated in the introduction. Two cases of the lower boundary will be discussed, a fixed end and a free end at the depth level $n+1$ where the horizontal rope is provided. The reason is due to the uncertainty of the actual boundary condition at this point. The actual boundary may be between the two cases.

For a line of length l ft., with weight W lbs./ft., the model consists of n equal masses $m = Wd/g$, where $d = \dfrac{l}{n+1}$ ft. is the equal interval between lumped masses, and $g = 32.2$ ft./sec.^{2}, the gravity constant. For the case of free vibration with small lateral displacements y_i ft., the deflected position and the free body diagram

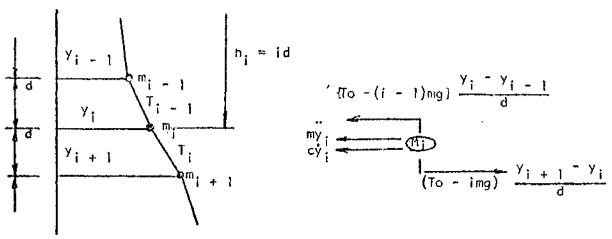

Fig. 5 Free Body Diagram of ith Mass

of the ith mass is shown in Fig. 5.

For the ith mass, $\dot{y}_i$ and $\ddot{y}_i$ are velocity in ft./sec. and acceleration in ft./sec.^{2} respectively. It is assumed that all masses are subjected to equal linear viscous damping C lbs.-sec./ft. For the case of free vibration resulting from an initial displacement, the dynamic equilibrium equation is

$$\ddot{y}_i+2\alpha\dot{y}_i-\frac{n\beta-i+1}{\lambda}y_{i-1}+\frac{2n\beta-2i+1}{\lambda}y_i-\frac{n\beta-i}{\lambda}y_{i+1}=0 \qquad \text{for} \quad i=1,2,\cdots,n \tag{12}$$

where

$$\alpha=\frac{c}{2m}\ \text{1/sec.}$$

$$\beta=\frac{T_0}{nmg}=\frac{T_a+nmg}{nmg}$$

T_0=the rope tension at the top boundary

T_a=the rope tension at the bottom boundary

and $\lambda=d/g$ sec.^{2}

We note that the bottom tension $T_a=0$ condition corresponds to the free end condition since there is no constraint force from the line below this bottom mass. In this case, we have $\beta=1$. Eq. (12) can be put in matrix form and for a special case of no damping, the matrix equation is

$$\underline{\ddot{Y}}+\boldsymbol{K}\underline{Y}=0 \tag{13}$$

where the accelerations and deflections are $n\times 1$ column matrices,

$$\underline{\ddot{Y}}=\{\ddot{y}_1, \ddot{y}_2, \cdots, \ddot{y}_n\} \tag{14}$$

and

$$\underline{Y}=\{y_1, y_2, \cdots, y_n\} \tag{15}$$

$\{\ \ \}$ indicates a column matrix.

The stiffness matrix is an $n\times n$ skewed diagonal matrix with three elements per row,

$$\boldsymbol{K}=\begin{bmatrix} \frac{2n\beta-1}{\lambda} & \frac{-n\beta+1}{\lambda} & 0\cdots\cdots\cdots\cdots\cdots 0 & & & \\ 0\cdots 0 & \frac{-n\beta+i-1}{\lambda} & \frac{2n\beta-2i+1}{\lambda} & \frac{-n\beta+i}{\lambda} & 0\cdots\cdots 0 \\ 0\cdots\cdots\cdots\cdots\cdots\cdots\cdots\cdots 0 & & & \frac{-n\beta+n-1}{\lambda} & \frac{2n\beta-2n+1}{\lambda} \end{bmatrix}. \tag{16}$$

Let

$$\underline{Y}=\boldsymbol{\Phi}\underline{\xi} \tag{17}$$

where

$$\boldsymbol{\Phi}=\begin{bmatrix} \phi_{11}, \phi_{12}, \cdots, \phi_{ij}, \cdots \\ \phi_{21}, \phi_{22}, \cdots \\ \phi_{i1}, \phi_{i2}, \cdots, \phi_{ij}, \cdots \\ \phi_{n1}, \phi_{n2}, \cdots\cdots\cdots, \phi_{nn} \end{bmatrix}=[\underline{\phi_1}, \underline{\phi_2}, \cdots, \underline{\phi_j}, \cdots, \underline{\phi_n}] \tag{18}$$

is the $n \times n$ transformation matrix termed as the mode shape matrix and,

$$\underline{\xi}=\{\xi_1, \xi_2, \cdots, \xi_i, \cdots, \xi_n\} \tag{19}$$

is the $n \times 1$ generalized coordinate matrix.

Introducing Eq. (17) in Eq. (13) and premultiplying the result by $\boldsymbol{\Phi}^{-1}$, we have

$$\ddot{\underline{\xi}}+\boldsymbol{\Phi}^{-1}\boldsymbol{K}\boldsymbol{\Phi}\underline{\xi}=0. \tag{20}$$

For a matrix equation of the form (20), the eigen values and eigen functions of the matrix $\boldsymbol{K}$ are the modal natural frequencies and corresponding mode shapes respectively. If the $\boldsymbol{K}$ matrix (16) is known, a computer routine is available to provide both the mode shape matrix and the modal natural frequency matrix as follows:

$$\boldsymbol{\Phi}=[\underline{\phi}_1, \underline{\phi}_2, \cdots, \underline{\phi}_j, \cdots, \underline{\phi}_n] \tag{21}$$

where

$$\underline{\phi}_j=\{\phi_{1j}, \phi_{2j}, \cdots, \phi_{ij}, \cdots, \phi_{nj}\} \tag{22}$$

and

$$\boldsymbol{\omega}_n{}^2=\boldsymbol{\Phi}^{-1}\boldsymbol{K}\boldsymbol{\Phi}=\begin{bmatrix} \omega_1{}^2 & & & & \\ & \omega_2{}^2 & & & \\ & & \ddots & & \\ & & & \omega_i{}^2 & \\ & & & & \ddots \\ & & & & & \omega_n{}^2 \end{bmatrix} \tag{23}$$

where $\omega_i{}^2$ is the squared natural frequency of the ith mode.

By using Eqs. (21) and (23), we can solve the damped system equations for the case of a sinusoidal load $F_j(t)=e^{i\omega t}$ at any point j. The resulting output solution element

$$y_i(t)=H_{ij}(\omega)e^{i\omega t} \tag{24}$$

provides the element $H_{ij}(\omega)$ of the frequency response function matrix $\boldsymbol{H}(\omega)$.

Starting with the forced vibration equation of the damped system,

$$\ddot{\underline{Y}}+2\alpha\dot{\underline{Y}}+\boldsymbol{K}\underline{Y}=\frac{1}{m}\underline{f}(t) \tag{25}$$

where the $n \times 1$ forcing function matrix is of the special form

$$\underline{f}(t)=\underline{f}_j e^{i\omega t} \tag{26}$$

and

$$f_i=\{0, 0, \cdots, 1, \cdots, 0\}, \qquad 1 \text{ at } j\text{th row} \tag{27}$$

the output element will be

$$y_i(t)=H_{ij}(\omega)e^{i\omega t} \qquad \text{such that}$$

$$\underline{Y}=\underline{H}e^{i\omega t} \tag{28}$$

where

$$\underline{H}_j=\{H_{1j}(\omega), H_{2j}(\omega),\cdots, \underline{H}_{nj}(\omega)\}. \tag{29}$$

Introducing Eqs. (26) and (28) into Eq. (25), we have

$$(-\omega^2\boldsymbol{I}+2i\alpha\omega\boldsymbol{I}+\boldsymbol{K})\boldsymbol{\Phi}\underline{\xi}=\frac{1}{m}\underline{f}_j e^{i\omega t} \tag{30}$$

where we used the relationship (17) and $\boldsymbol{I}$ is a unit matrix. Premultiplying Eq. (30) by $\boldsymbol{\Phi}^{-1}$, we obtain

$$\underline{\xi}=\frac{1}{m}\boldsymbol{H}_0(\omega)\boldsymbol{\Phi}^{-1}\underline{f}_j e^{i\omega t} \tag{31}$$

where

$$\boldsymbol{H}_0(\omega)=(-\omega^2\boldsymbol{I}+2i\alpha\omega\boldsymbol{I}+\boldsymbol{\omega}_n^2)^{-1} \tag{32}$$

$\boldsymbol{H}_0(\omega)$ is the inverse of an $n\times n$ diagonal matrix and therefore it is also an $n\times n$ diagonal matrix with elements

$$H_{0ii}(\omega)=\frac{1}{\omega_i^2-\omega^2+2i\alpha\omega}. \tag{33}$$

This expression is identical to the frequency response function for a single degree of freedom system with harmonic frequency ω_i.

Premultiplying Eq. (31) by $\boldsymbol{\Phi}$ and using Eqs. (17) and (28), we obtain for $\underline{H}_j(\omega)$

$$\underline{H}_j(\omega)=\frac{1}{m}\boldsymbol{\Phi}\boldsymbol{H}_0(\omega)\boldsymbol{\Phi}^{-1}\underline{f}_j. \tag{34}$$

If we denote the element of the $n\times n$ inverse matrix $\boldsymbol{\Phi}^{-1}$ by θ_{ij}, the general form of the ith element $H_{ij}(\omega)$ of the $n\times 1$ H_j matrix is

$$H_{ij}(\omega)=\frac{1}{m}\sum_{k=1}^{n}\sum_{p=1}^{n}\sum_{q=1}^{n}\phi_{ik}H_{0kp}(\omega)\theta_{pq}f_{qj}. \tag{35}$$

With the conditions $f_{qj}=1$ for $q=j$ and 0 for $q\neq j$, and $H_{0kp}(\omega)=H_{0kk}(\omega)$ for $k=p$ and 0 for $k\neq p$, Eq. (35) is simplified into

$$H_{ij}(\omega)=\frac{1}{m}\sum_{k=1}^{n}\phi_{ik}H_{0kk}(\omega)\theta_{kj} \tag{36}$$

physical interpretation of $H_{ij}(\omega)$ is its description of the output at location i, $y_i(t)=H_{ij}(\omega)e^{i\omega t}$ when the input is the force $F_j(t)=e^{i\omega t}$ at location j, for $i, j=1$ to n.

With Eq. (36), $\boldsymbol{H}(\omega)$ matrix with elements $\boldsymbol{H}_{ij}(\omega)$ can be made as follows

$$\boldsymbol{H}(\omega)=\begin{bmatrix} H_{11}(\omega),\cdots, H_{ij}(\omega),\cdots & \\ H_{i1}(\omega),\cdots, H_{ij}(\omega),\cdots & \\ H_{n1}(\omega),\cdots & H_{nn}(\omega) \end{bmatrix}. \tag{37}$$

This $\boldsymbol{H}(\omega)$ matrix is the frequency response function matrix for the vertical line system and is needed for the reliability analysis which follows next.

IV. RELIABILITY OF THE SYSTEM

It is well known that for the given cross-spectral density function of the turbulence force $\boldsymbol{S}_f$, Eq. (9) and for the vertical line system frequency response function $\boldsymbol{H}(\omega)$, Eq. (37), the $n \times n$ cross-spectral density matrix of lateral displacement is given by[3]

$$\boldsymbol{S}_y = \boldsymbol{H}(\omega)\boldsymbol{S}_f\boldsymbol{H}^{*\prime}(\omega) \tag{38}$$

where $\boldsymbol{H}^{*\prime}(\omega)$ is a transposed, complex conjugate matrix of $\boldsymbol{H}(\omega)$.

From the theory of random processes[4], when the input to a linear system is a stationary normal process, then the output is also a stationary normal process. Therefore, the lateral displacement output $y_i(t)$ at any location $i=1, 2, \cdots, n$ is a stationary normal process with a spectral density function $\boldsymbol{S}_y$ given by Eq. (38).

According to our criteria of the safe operation, the failure will be defined by the probability that any two out of the three lines entangle during a specified time. However, for the conservative estimation, we define the reliability (non-failure probability) by a probability that the stationary normal process of $y(t)$ remains below a positive level, D which is the spacing between the ocean surface ends of lines during a time period T.

Due to Crandall[4], this reliability is given by

$$R = \exp\{-NT\} \tag{39}$$

where

$$N = \frac{1}{\pi}\frac{\sigma_y'}{\sigma_y}\exp\left(-\frac{D^2}{2\sigma_y^2}\right) \tag{40}$$

and

$$\sigma_y' = \left[\int_{-\infty}^{\infty} \omega^2 S_{yii}(\omega)d\omega\right]^{1/2} \tag{41}$$

$$\sigma_y = \left[\int_{-\infty}^{\infty} S_{yii}(\omega)d\omega\right]^{1/2} \tag{42}$$

$S_{yii}(\omega)$ is an ith diagonal component of matrix $\boldsymbol{S}_y$ and is given by pre-multiplying Eq. (38) by an $n \times n$ unit matrix $\boldsymbol{I}$ as follows.

$$S_{yii}(\omega) = \sum_{p=1}^{n}\sum_{q=1}^{n} H_{ip}(\omega)H_{qi}^{*\prime}(\omega)\,. \tag{43}$$

If we perform the integrations in the right hand side of Eqs. (41) and (42) together with Eq. (43), replacing $S_{pq}(\omega)$ by the discrete form, Eq. (11) we have

$$\sigma_y^{2\prime} = \sum_{p=1}^{n}\sum_{q=1}^{n}\sum_{k=1}^{n}\sum_{r=1}^{n} \frac{1}{m^2}\phi_{ik}\phi_{ir}\theta_{kp}\theta_{rp}J(N, k, p, q, r) \tag{44}$$

and

$$\sigma_y^2 = \sum_{p=1}^{n}\sum_{q=1}^{n}\sum_{k=1}^{n}\sum_{r=1}^{n} \frac{1}{m^2}\phi_{ik}\phi_{ir}\theta_{kp}\theta_{rp}K(N, k, p, q, r) \tag{45}$$

where

$$J(N,k,p,q,r)=2\sum_{t=1}^{N}\omega_t^2 S_{pq}(\omega_t)\Delta\omega\frac{(\omega_k^2-\omega_t^2)(\omega_r^2-\omega_t^2)+4\alpha^2\omega_t^2}{[(\omega_k^2-\omega_t^2)(\omega_r^2-\omega_t^2)+4\alpha^2\omega_t^2]^2+4\alpha^2\omega_t^2(\omega_r^2-\omega_k^2)^2} \quad (46)$$

and

$$K(N,k,p,q,r)=2\sum_{t=1}^{N}S_{pq}(\omega_t)\Delta\omega\frac{(\omega_k^2-\omega_t^2)(\omega_r^2-\omega_t^2)+4\alpha^2\omega_t^2}{[(\omega_k^2-\omega_t^2)(\omega_r^2-\omega_t^2)+4\alpha^2\omega_t^2]^2+4\alpha^2\omega_t^2(\omega_r^2-\omega_k^2)^2}\,. \quad (47)$$

The reliability, Eq. (39) may be calculated for any given vertical line system, with specified T and D, and turbulence described by $S_f(\omega)$.

The safe top spacing, D corresponding to a given level of safety, or reliability R is expressed from Eqs. (39) and (40) as follows.

$$D=\sqrt{2\sigma_y^2\ln\left[-\frac{T}{\pi}\frac{\sigma_y'}{\sigma_y}\frac{1}{\ln R}\right]}\,. \quad (48)$$

If it is required that D be two-sided (for the case where a middle vertical line may entangle with guide lines on either side), then we use

$$N_2=2N \qquad \text{in Eq. (40).} \quad (49)$$

V. APPLICATION

The numerical example is given here in order to demonstrate the application of the developed theory. The input data are listed in Table 1.

For the numerical example, we used $\omega_c=5$ rad./sec. and $\Delta\omega=\frac{\omega_c}{5}=1$ rad./sec. This ω_c value will cause excitation of the important system modes and represents a reasonable cut-off frequency for highest possible subsurface turbulence due to post strom sea conditions. The $\Delta\omega$ is small enough to both describe the spectral density functions and provide sufficient accuracy of numerical integration. The

Table 1 Input Data

Parameters	Explanation	Numerical values
n	Selected number of discrete masses	5
α (1/csc.)	$=\frac{c}{2m}$; damping ratio	0.8
β	$=\frac{T_a+nmg}{nmg}$; tension ratio	4.0
l (ft.)	vertical line length	500, 5000, 15000
λ (sec.^{2})	$=\frac{d}{g}=\frac{l}{(n+1)g}$; spacing ratio	2.59, 25.9, 77.9
B	turbulence parameters	1.0
D	turbulence parameters	1.0
G	turbulence parameters	1.0
C_{11} (lb.^{2})	top (at $i=1$) turbulence variance	$\frac{l^2}{(n+1)^2}$
ω_c (rad./sec.)	cut-off frequency	5
$m\left(\frac{\text{lb.}\cdot\text{sec.}^2}{\text{ft.}}\right)$	$=\frac{Wd}{g}$; point mass	$0.33\frac{l}{n+1}$

selected number of discrete masses is $n=5$. Assuming that the cable diameter is 2 inches (solid steel cable), we have $w=10.7$ lbs./ft. Thus, $m=\frac{10.7}{32.2}$, $d=0.33\frac{l}{n\times 1}$. Estimating the root mean squared value of the turbulence force as $q=1$ lb./ft. (no data available, hence this is a pure estimation), C_{11} will be $C_{11}=(qd)^2=d^2=\frac{l^2}{(n+1)^2}$.

Table 2 Allowable Space D with 99% Reliability for $T=100$ Hours Duration (Two-sided)

l	D for fixed lower boundary	D for free lower boundary
500 ft.	2.8 ft.	10.6 ft.
5 000	11.9	32.4
15 000	20.8	36.4

Table 2 gives the absolute (two-sided) 99% reliable bound D in feet for the time duration $T=100$ hours of the turbulence at the critical location of the cable for two different lower boundary conditions. For example, we can say that if the cable length is $l=5\,000$ ft. with fixed lower boundary, the top spacing $D=11.9$ ft. gives the 99% two-sided reliability of the system for 100 hours time duration.

VI. CONCLUSIONS

The method of estimating the safe spacing between the top surface ends of the cable system is presented and the numerical example was given for the application. The problem is really of two parts, one is the formulation of turbulence force field and the other is the dynamic analysis of the system. With no data available, the model for the variance and covariance of turbulence force (Fig. 3) may not reflect the actual phenomena and should be improved by collecting the proper data. As for the excitation forces, only the turbulence force was considered. However, we note that the entanglement can occur due to the vertical motion of the ocean surface. When the frequency of the sinusoidal variation in the rope tension coincides with the harmonic frequency of one or more of the lines, this may cause a severe displacement of the lines. Largely different responses of the three cables may also occur due to the constant current force. However, these cases may be eliminated. For example, as to the vertical motion, a change in tension of the lines can change the system frequency. As to the current force, nearly equal tensions and weights should be employed as suggested in the introduction.

The lengthy equations involved in the dynamic analyses can be easily treated by a digital computer.

Although the study presented herein was theoretical due to the lack of data, it will serve as engineering information for the design of such a system.

REFERENCES

1) Zsutty, T.: "Study of Entanglement Probability Among Long Vertical Lines in Ocean," Aug., 1969, Tech. Report, Naval Civil Eng. Lab., Port Hueneme, California.
2) Darling, R. C.: "Cable Length Determinations for Deep Sea Oceanographic Operation," Tech. Bulletin No. 30, U.S. Environmental Science Service Administration.
3) Lin, Y. K.: *Probabilistic Theory of Structural Dynamics*, McGraw Hill, New York, 1967.
4) Crandall, S. H. and Mark, W. D.: *Random Vibration in Mechanical Systems*, Academic Press, New York, 1963.

(*Received April 13, 1970*)